Entwined Planar Spirals for Artificial Surface

Vallecchi, A., & Schuchinsky, A. (2010). Entwined Planar Spirals for Artificial Surface. IEEE Antennas and Wireless Propagation Letters, 9, 994-997. [5599282]. DOI: 10.1109/LAWP.2010.2086424

Published in:
IEEE Antennas and Wireless Propagation Letters

Entwined Planar Spirals for Artificial Surfaces

Andrea Vallecchi and Alexander G. Schuchinsky, *Senior Member, IEEE*

***Abstract*—Entwining planar quadrifilar spirals arranged in doubly periodic arrays enables a strong subwavelength response of the unit cell smaller than 1/40 of wavelength. It is shown that interleaving counterwound spiral arms extended into adjacent unit cells dramatically increases the equivalent capacitance while reducing the inductance. The dielectric substrate enhances this effect of the unit cell miniaturization with concurrent bandwidth expansion. The proposed topology of compact planar spiral array exhibits excellent angular and polarization stability and circular polarization selectivity in a broad frequency band. Negligible variations of the resonance frequency are demonstrated for both TE and TM polarized waves at incidence angles up to 45° with a common fractional bandwidth over 40% at the level of −10 dB.**

***Index Terms*—Artificial surfaces, electromagnetic band-gap (EBG), periodic structures, planar spirals.**

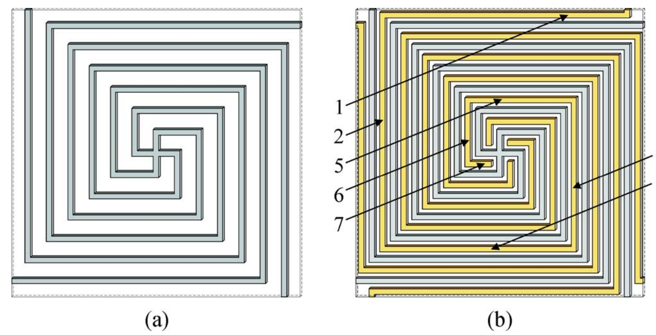

Fig. 1. Unit cell of the doubly periodic array of quadrifilar spirals: (a) basic spiral; (b) entwined spirals containing up to seven interleaved segments of the spiral conductors extended from the surrounding cells. The external spiral arms are open-ended at the unit cell center (*color online*).

I. Introduction

Artificial surfaces composed of arrays of periodically patterned conductors have ubiquitous applications in low-profile antennas, high impedance surfaces (HISs), frequency selective surfaces (FSSs), spatial filters, and radomes, to mention a few. To attain strong resonance response of such arrays, the physical size of their individual constituent elements and unit cells are usually required to be commensurate with half a wavelength. This imposes stringent constraints on integration of such artificial surfaces with RF front-ends, small mobile terminals, and conformal antennas.

Several approaches have been proposed to reduce the unit cell size. In [1], conductor patches have been complemented by stripes on the back of substrate to introduce strong reactive couplings, which decrease the resonance frequency of the unit cell. A similar effect has been achieved with the use of lumped inductive and capacitive elements in [2], while not relying on resonance effects of the FSS geometry. An alternative concept based upon space-filling curves has been applied to arrays of convoluted linear and crossed dipoles [3]–[5]. These types of constituent elements provide smaller unit cell size and also demonstrate improved stability of the array response to waves incident at different angles. However, miniaturization of the unit cells with closely spaced resonance elements often entails degradation of the FSS performance and prohibitively narrows fractional bandwidth[1] (FBW). To alleviate these drawbacks, it has recently been suggested to extend each array element beyond a single unit cell by interweaving the conductor patterns in adjacent unit cells. This approach leads not only to reducing the unit cell size, but also to broadening the array operational bandwidth [6]. By expanding the arms of meandered crossed dipoles [4] and interweaving their fingers in adjacent cells, a wideband FSS with miniaturized unit cell has been demonstrated in [7].

In this letter, we propose a new topology of a planar array comprised of entwined quadrifilar spirals that enables 40% reduction of the unit cell size as compared to that for the interwoven convoluted crossed dipoles [7]. The array of entwined spirals extended into adjacent unit cells provides the resonance response at frequencies 20 times lower than those for nonconvoluted crossed dipoles with the same unit cell size. The entwined spirals also exhibit superior performance in dual-polarized operation with very low cross-polarization levels and naturally provide a high polarization purity response to circularly polarized fields.

The principle of spiral intertwining and the features enabled by the proposed new geometries are discussed in this letter by the example of quadrifilar spirals arranged in a doubly periodic array with square lattice.

II. Arrays of Entwined Planar Spirals

The constitutive unit cells of a doubly periodic array comprised of the (a) basic and (b) entwined quadrifilar spirals are shown in Fig. 1. The entwined spirals are formed by counter-winding the external spiral arms extended from the surrounding unit cells in the gaps between the arms of the reference basic spiral.

Manuscript received August 01, 2010; revised October 04, 2010; accepted October 05, 2010. Date of publication October 11, 2010; date of current version November 04, 2010. This work was supported in part by the EU FP7 project ECONAM under Grant 218696.

A. Vallecchi is with the Department of Information Engineering, University of Siena, Siena 53100, Italy (e-mail: andrea.vallecchi@unisi.it).

A. G. Schuchinsky is with the Institute of Electronics, Communications and Information Technology, School of Electrical and Electronic Engineering and Computer Science, Queen's University of Belfast, Belfast BT3 9DT, U.K. (e-mail: a.schuchinsky@qub.ac.uk).

Color versions of one or more of the figures in this letter are available online at http://ieeexplore.ieee.org.

Digital Object Identifier 10.1109/LAWP.2010.2086424

[1]The fractional bandwidth is defined in this letter as the rejection band width at the transmission level −10 dB, normalized to the resonance frequency.

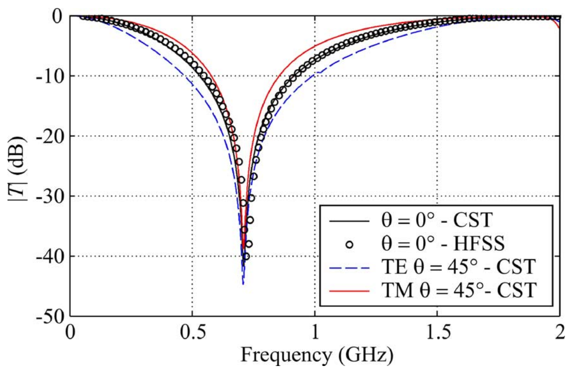

Fig. 2. Transmittance of the fully entwined quadrifilar spiral array, Fig. 1(b), at normal and oblique incidence of TE and TM waves. The results from CST and HFSS simulators are compared for normal incidence only.

TABLE I
RESONANCE FREQUENCIES AND FBW FOR DIFFERENT ARRAY PATTERNS WITH SQUARE LATTICE PERIODICITY $p = 10.8$ mm

	f_r (GHz)	λ_r/p	Frequency offset (%)		FBW (%)		
Incidence	Normal	Normal	TE at 45°	TM at 45°	Normal	TE at 45°	TM at 45°
X-dipoles [7]	14.7	1.88	−7.9	3.7	12	11	7.7
Interwoven X-dipoles [7]	1.00	27.8	0.2	−0.2	63	85	46
Quadrifilar spiral	2.18	12.7	0.01	0.06	2.75	3.7	1.9
7-Fold entwined spiral	0.71	39	0.05	−0.1	55	74.5	40
7-Fold entwined spiral on 1.6-mm-FR4 substrate	0.43	64	0	−0.2	82.5	108	61.2

The infinite doubly periodic spiral arrays have been modeled using a single unit cell bounded by the periodic boundary conditions. The periodicity $p = 10.8$ mm of the square lattice and width of the spiral conductors and gaps equal to 0.2 mm in the fully entwined spirals have been chosen the same as in [7] to allow for consistent comparison to the FSS composed of the interwoven convoluted crossed dipoles. The spiral conductors have finite thickness of 17.5 μm.

The transmission and reflection characteristics of the entwined spiral array have been simulated in CST Microwave Studio and validated with Ansoft HFSS. The results obtained by these two simulators, based upon entirely different methods, are in full agreement, as illustrated in Fig. 2.

The quadrifilar spiral, shown in Fig. 1(a), represents a canonical geometry of convoluted conductors, which enables significant reduction of the unit cell size and improves angular stability of the array performance. However this structure exhibits very narrow band response, as indicated in Table I. This behavior of the spiral array can be understood with the aid of a simple circuit model, which is commonly used for the FSS analysis [8]. Indeed, a unit cell of periodically arranged spirals may be represented as a transmission line loaded with a shunt reactance composed of inductance L and capacitance C connected in series. Then, frequency of the rejection resonance, producing the transmission null, is expressed as $f_{\rm r} \sim 1/\sqrt{LC}$, and the respective fractional bandwidth is $B_n \sim \sqrt{C/L}$ [6]. Although this simple LC model gives only a basic description of the arrays with complex unit cell geometries, such as quadrifilar spirals, it allows a fairly accurate estimate of the array response near the fundamental resonance and provides qualitative insight into the principal features of the spirals' resonance performance as detailed in Section III.

From the full-wave simulations of planar spirals, it is known that the length of the spiral conductor mainly contributes to equivalent inductance, while respective capacitance remains practically unchanged, being primarily determined by the coupling between adjacent turns. Then, according to the qualitative estimations above, $f_{\rm r}$ decreases as the spiral arms become longer and the respective FBW narrows.

To overcome the latter shortcoming of quadrifilar spiral arrays and further reduce the unit cell size, it has been proposed in [9] to entwine the reference spiral with the spiral arms extended from the surrounding unit cells. This is achieved by winding the spiral conductor arms protruding from the adjacent unit cells into the gaps between the turns of the basic spiral centered in the reference unit cell. The four additional conductors are thus counterwound inside the basic reference spiral as illustrated in Fig. 1(b) and provide efficient concurrent control of both the equivalent capacitance and inductance in the unit cell. As a result, the entwined spiral geometry enables further significant reduction of the unit cell electrical size along with broadening FBW at ever lower resonance frequencies.

III. EFFECT OF SPIRAL INTERTWINING

Let us now examine the mechanisms underlying the distinctive properties of the entwined spiral arrays. The transmittance (T) and reflectance (R) for a normally incident wave are shown in Fig. 3 at variable lengths of the interleaved conductor arms extended from the surrounding cells into the basic spiral in the reference unit cell. At $N = 1$, only straight segments labeled "1" in Fig. 1(b) are present at each side of the basic quadrifilar spiral, while at $N = 7$, all seven folds of the extended conductors fill all the slots between the turns of the reference basic spiral.

The effect of the number of intertwined folds on resonance frequency $f_{\rm r}$ and FBW of the fundamental mode is shown in Fig. 4. As the number of intertwined folds increases, FBW grows and $f_{\rm r}$ decreases monotonically, though at a progressively slower rate. For the fully entwined 7-fold spirals, $f_{\rm r} = 0.71$ GHz and FBW reaches 55%. This corresponds to the packaging density[2] of $\lambda_{\rm r}/p = 39$, which is 40% higher than

[2]Packaging density is defined as the ratio of the resonance wavelength to the array periodicity, $\lambda_{\rm r}/p$.

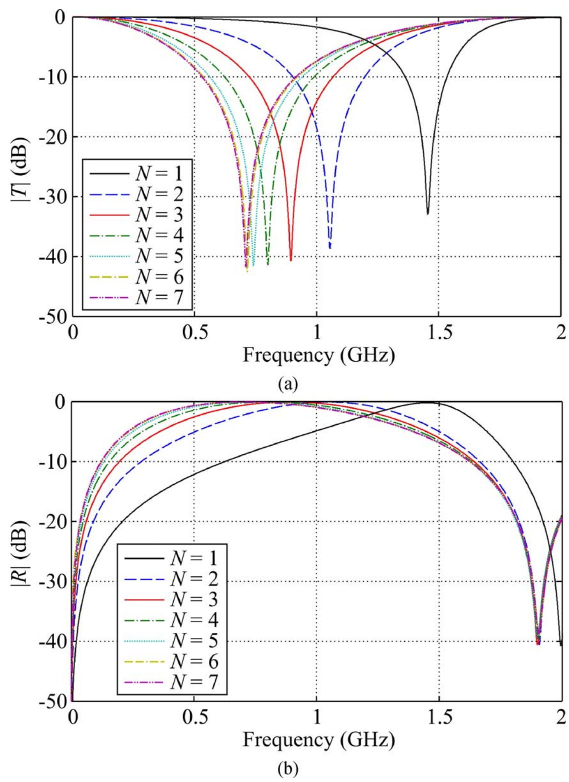

Fig. 3. (a) Transmittance and (b) reflectance of the entwined quadrifilar spiral array at variable number of intertwined folds.

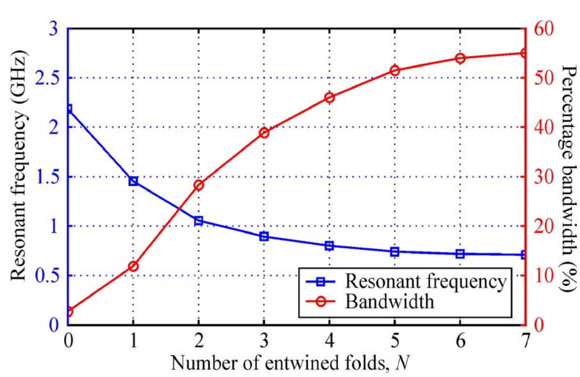

Fig. 4. Resonance frequency and FBW versus the number of intertwined folds in the reference quadrifilar spiral (CST simulations).

that for interwoven crossed dipoles [7] with the same lattice constant; $\lambda_{\rm r}$ is wavelength at frequency $f_{\rm r}$.

Such dramatic increase of $\lambda_{\rm r}/p$ in the entwined spirals is attributed to the large equivalent capacitance, which also provides broader FBW that is consistent with the LC model prediction. From the physical standpoint, a large capacitive content arises in the entwined spirals due to the conductor arms extended from the surrounding unit cells into the reference basic spiral and counterwound between its turns. Correspondingly, the coupling between the intertwined spiral conductors is distributed over their entire length. It adds up and increases the total unit cell capacitance, whereas the negative mutual inductance between the oppositely wound arms reduces the total equivalent inductance.

These features of the entwined spiral array are fully consistent with the basic LC model mentioned in Section II. Namely, the L and C parameters retrieved from the simulated array char-

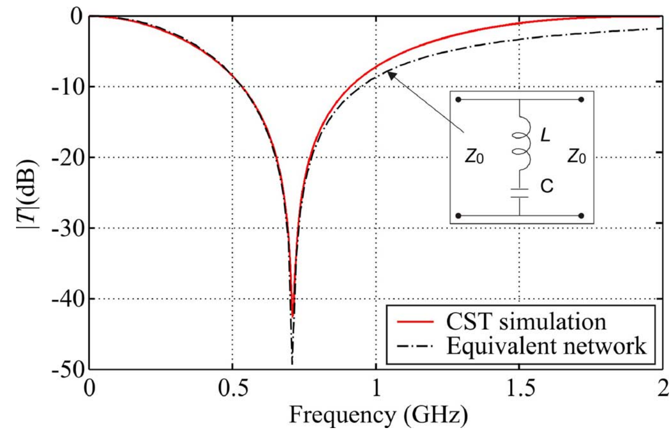

Fig. 5. Transmittance of the fully entwined 7-fold quadrifilar spiral array with period $p = 10.8$ mm: CST simulations (solid line) versus the equivalent LC circuit model with the retrieved $L = 23.98$ nH and $C = 2.0889$ pF (dash-dotted line).

acteristics have the values $L = 126.15$ nH, $C = 0.042$ pF and $L = 23.98$ nH, $C = 2.089$ pF for the basic and entwined quadrifilar spirals, respectively. Comparison of these L and C values confirms that the entwined spirals have much larger equivalent capacitance ($\sim$50 times that of the basic quadrifilar spiral), while their inductance is smaller ($\sim$5 times).

In order to further validate the LC model, the transmission characteristics of the fully intertwined spiral array with the unit cell of Fig. 1(b) have been simulated in CST Microwave Studio and compared to the LC model prediction over broad frequency band. The results in Fig. 5 display good agreement for the fundamental resonance mode, thus proving that the LC model provides adequate qualitative and quantitative descriptions of the array resonance response.

As demonstrated above, the capacitive coupling has a major impact on the performance of the freestanding entwined spiral arrays. Therefore, it is important to assess the effect of a dielectric substrate on the response of the entwined spirals. It is known that even a thin dielectric substrate causes lowering $f_{\rm r}$ of the FSS [8], [10]. The respective FBW slowly broadens as the substrate becomes thicker, but when thickness gets close to half a wavelength, FBW reduces due to the dielectric resonance [10]. The transmission and reflection responses of the entwined spiral array printed on FR4 substrate ($\varepsilon_r = 4.9$) of thickness 1.6 mm have been simulated in CST Microwave Studio for normal and oblique incidence of TE and TM waves. It can be observed in Fig. 6 that the resonance frequency ($f_{\rm r} = 0.43$ GHz) becomes lower than for the freestanding array. Thus, the packaging density rises to $\lambda_{\rm r}/p = 64$ (for the same lattice constant $p = 10.8$ mm), while the common FBW (limited by TM polarization) grows to $\sim 61\%$. This substantial increase of the FBW, being much larger than that obtained with the conventional dipole FSS [10], is again enabled by the spiral conductor pattern and its enhanced capacitive content. It is also noteworthy in Fig. 6 that the reflection losses in the entwined spiral array on FR4 substrate remain very low.

IV. Angular and Polarization Stability

The entwined spiral arrays simulated at oblique incidence have demonstrated high stability of their response in a broad

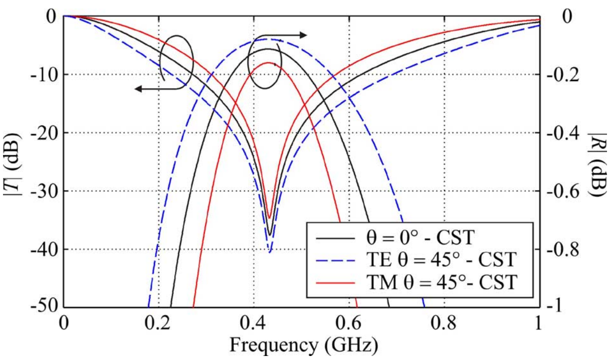

Fig. 6. Transmittance and reflectance of the entwined 7-fold quadrifilar spiral array on a 1.6-mm-thick FR4 substrate at normal and oblique incidence of TE and TM waves.

range of incidence angles. Figs. 2 and 6 show that the resonance frequencies for both TE and TM waves at normal and oblique, 45°, incidence are practically indistinguishable. This implies that the entwined spiral arrays are particularly apt for handling circular polarized waves while producing a negligible level of cross-polarization in the scattered field.

The characteristics of the fully entwined spiral arrays at normal and oblique incidence (freestanding and on dielectric substrate) are summarized in Table I in comparison to the respective data for nonconvoluted and fully interwoven convoluted crossed dipoles [7] and the basic quadrifilar spirals.[3] The presented results demonstrate the superior performance of the entwined spirals in terms of the angular and polarization stability at much lower resonance frequencies than those achievable with other configurations.

V. Conclusion

A novel topology of planar arrays comprised of entwined quadrifilar spirals has been proposed. It allows a remarkable reduction of the unit cell size while exhibiting excellent frequency stability of TE and TM resonances with a wide common FBW ($\sim 40\%$ for the freestanding arrays). Using the simple LC model, it is shown that the unique performance of the entwined spiral arrays is the result of significant increase of the equivalent capacitance and reduction of the equivalent inductance of the unit cell. These are achieved by virtue of the tight coupling between the counterwound spirals extended from the adjacent cells and interleaved inside each other.

The main distinctive features of the entwined spiral arrays can be summarized as follows.

— The packaging density of the freestanding entwined spiral arrays ($\lambda_{\mathrm{r}}/p \sim 40$) exceeds 1.4 times that for the interwoven convoluted crossed dipoles [7] and 3 times that for the basic quadrifilar spirals.

[3]Further comparison for the partly intertwined spirals is provided in [9].

— Introduction of dielectric substrate further increases the unit cell miniaturization. For low-cost FR4 substrate, the packaging density grows to $\lambda_{\mathrm{r}}/p = 64$, while FBW reaches 61.2% with low reflection loss for a TM wave incident at 45°.

— The resonance frequency offset between TE and TM waves incident at 45° is considerably smaller than that attainable with the interwoven convoluted crossed dipoles [7].

— The entwined spiral arrays exhibit excellent polarization and angular stability for TE, TM, and circular polarizations with low level (below -50 dB at normal incidence) of cross polarization.

The small unit cell size and angular stability of the array response make the entwined spirals attractive for applications in miniaturized spatial filters, and conformal reflectors and high impedance surfaces for low-profile antennas mounted on mobile terminals. Owing to the extremely small subwavelength size of the unit cell, the entwined multifilar spirals may be particularly suitable for the design of homogeneous metamaterials and metasurfaces.

Finally, it is noteworthy that the concept of interleaving planar spirals is not limited to quadrifilar spirals, but is also applicable to the spiral arrays with other lattice symmetries and the complementary spiral layouts.

References

[1] K. Sarabandi and N. Behdad, "A frequency selective surface with miniaturized elements," *IEEE Trans. Antennas Propag.*, vol. 55, no. 5, pp. 1239–1245, May 2007.

[2] H. Liu, K. L. Ford, and R. J. Langley, "Miniaturised bandpass frequency selective surface with lumped components," *Electron Lett.*, vol. 44, no. 18, pp. 1054–1055, Aug. 2008.

[3] E. A. Parker and A. N. A. El Sheikh, "Convoluted array elements and reduced size unit cells for frequency-selective surfaces," *Proc. Microw., Antennas Propag.*, vol. 138, pp. 19–22, Feb. 1991.

[4] E. A. Parker, A. N. A. El Sheikh, and A. C. de C. Lima, "Convoluted frequency-selective array elements derived from linear and crossed dipoles," *Proc. Microw., Antennas Propag.*, vol. 140, pp. 378–380, Oct. 1993.

[5] C. R. Simovski, P. de Maagt, S. A. Tretyakov, M. Paquay, and A. A. Sochava, "Angular stabilization of resonant frequency of artificial magnetic conductors for TE-incidence," *Electron. Lett.*, vol. 40, no. 2, pp. 92–93, Jan. 2004.

[6] S. Barbagallo, A. Monorchio, and G. Manara, "Small periodicity FSS screens with enhanced bandwidth performance," *Electron. Lett.*, vol. 42, pp. 382–384, Mar. 2006.

[7] F. Huang, J. C. Batchelor, and E. A. Parker, "Interwoven convoluted element frequency selective surfaces with wide bandwidths," *Electron. Lett.*, vol. 42, pp. 788–790, Jul. 2006.

[8] B. A. Munk, *Frequency Selective Surfaces: Theory and Design*. New York: Wiley, 2000.

[9] A. Vallecchi and A. G. Schuchinsky, "Entwined spirals for ultra compact wideband frequency selective surfaces," in *Proc. EuCAP*, Barcelona, Spain, Apr. 12–16, 2010, A18P2-5.

[10] P. Callaghan, E. A. Parker, and R. J. Langley, "Influence of supporting dielectric layers on the transmission properties of frequency selective surfaces," *Proc. Microw., Antennas Propag.*, vol. 138, no. 5, pp. 448–454, Oct. 1991.